Supporting Online Material for

Logic of the Yeast Metabolic Cycle: Temporal Compartmentalization of Cellular Processes

Benjamin P. Tu, Andrzej Kudlicki, Maga Rowicka, Steven L. McKnight*

*To whom correspondence should be addressed. E-Mail: smckni@biochem.swmed.edu

Published 27 October 2005 on *Science* Express
DOI: 10.1126/science.1120499

This PDF file includes:

SUPPORTING ONLINE MATERIAL

(Tu, B.P., Kudlicki, A., Rowicka, M., McKnight, S.L. Logic of the Yeast Metabolic Cycle: Temporal Compartmentalization of Cellular Processes)

Our microarray data and supporting data files are accessible at http://yeast.swmed.edu

MATERIALS AND METHODS

Yeast strains and methods

Yeast manipulations were performed using standard methods (*1*). The CEN.PK122 diploid strain was kindly provided by P. Kötter. CEN.PK diploid strains containing C-terminally GFP-tagged proteins were constructed using oligonucleotide-directed homologous integration of a GFP-Kan^R cassette (*2*). Following recovery at 30° for a minimum of 6 h, integrants were selected on YEPD plates containing 200 µg/mL G418 sulfate and verified by PCR and visualization. For FACS analysis, cells were processed and stained with propidium iodide as described previously (*3*).

Continuous culture conditions

Fermentors were from New Brunswick Scientific (Model BioFlo 110). Each fermentor run was started by the addition of a 10-20 mL starter culture that had been grown overnight to saturation at 30°. The fermentors were operated at an agitation rate of 400 rpm, an aeration rate of 1 L/min, a temperature of 30°, a pH of 3.4, with a working volume of 1 L. Once the batch culture reached maximal density, the culture was starved for a minimum of 4 h. Continuous culture was then initiated by the constant infusion of media containing 1% glucose at a dilution rate of ~0.09-0.1 h^{-1}. The growth media is a minimal media consisting of 5 g/L $(NH_4)_2SO_4$, 2 g/L KH_2PO_4, 0.5 g/L $MgSO_4 \cdot 7H_2O$, 0.1 g/L $CaCl_2 \cdot 2H_2O$, 0.02 g/L $FeSO_4 \cdot 7H_2O$, 0.01 g/L $ZnSO_4 \cdot 7H_2O$, 0.005 g/L $CuSO_4 \cdot 5H_2O$, 0.001 g/L $MnCl_2 \cdot 4H_2O$, 1 g/L yeast extract, 10 g/L glucose, 0.5 mL/L 70% H_2SO_4, and 0.5 mL/L Antifoam 204 (Sigma). Using IFO0233, another prototrophic, diploid strain of *S. cerevisiae* (*4*), we were also able to observe cycles with period ~4-5 h (*5*). CEN.PK haploids also exhibited metabolic cycles similar to those of the diploid parent (*5*). However, under the same fermentor conditions, we failed to observe metabolic cycling with the common laboratory strains S288C and W303 (*5*). These strains have been domesticated and engineered to possess auxotrophic metabolic markers that likely impede metabolic oscillation.

RNA preparation and microarray analysis

Approximately 2 x 10^8 cells per time interval were rapidly harvested from the fermentor and frozen at -80°. The first time interval of a cycle typically was chosen to be the very beginning of reductive phase when dissolved oxygen levels are rising most rapidly. Yeast total RNA was prepared using an Ambion RiboPure-Yeast Kit (Ambion, Inc.). RNA quality was confirmed by A_{260}/A_{280} ratio (>2.0) and Agilent Bioanalyzer analysis (28S:18S = 1.5-2.0) before further processing. All arrays were YG_S98

oligonucleotide arrays (Affymetrix, Inc.). cDNA synthesis, cRNA labeling, hybridization, and scanning were performed according to the manufacturer's instructions (Affymetrix). The raw data were initially analyzed using GeneChip Operating Software (GCOC) v1.1 (Affymetrix). Then data sets from comparison files were imported into Excel (Microsoft) and Genespring v7 (Silicon Genetics) as well as software developed in-house specifically for this project for further comparative analysis. We classified those probes that had at least 3 (on average one per cycle) 'present' (P) calls (as generated by Affymetrix GeneChip software) as expressed. According to this criterion, out of 9,335 probes queried by the YG_S98 array, 7,985 (~86%) were expressed. Out of 6,555 probes querying unique, annotated ORFs, 6,209 were expressed. Among these, our autocorrelation-based periodicity analysis detected 3,552 ORFs periodic with confidence level of 95% or better (Table 1).

Periodicity analysis

To date, the problem of detecting periodic transcripts has been encountered in both studies of the cell cycle and circadian rhythm. No consensus periodicity detection method has been reached in either of those fields (*6, 7*). In contrast to other studies, in our approach the primary determinant of periodicity is the autocorrelation of the transcript temporal profile. Our method is the most appropriate for data sampled with a high temporal resolution. The first step in our analysis was calculating the consensus period and confirming that it coincides with the ~5 h metabolic oscillations. For each gene, we first calculated a Lomb periodogram, which is a non-biased estimator of the periodogram for unevenly spaced data (*8, 9*) and, for a range of possible periods, assessed the probability that the gene is periodic (*10*). From this, we combined the data for all genes in a maximum likelihood analysis, yielding a most probable period of 299.86 min (~300 min). This confirmed that many genes in our study are expressed in a periodic manner reflecting the period of the dissolved oxygen oscillations. However, to identify individual transcripts whose expression follows the ~300 min period, we choose a method based on calculating autocorrelation function (ACF), rather than the Fourier-based periodogram method. The reason for this lies in the high quality of data, especially their extraordinary temporal resolution: we have gathered data for 12 time intervals/cycle, while in other studies fewer data points per cycle were available (*11, 12*). Due to this high resolution, we can detect a number of temporal profiles that cannot be seen by Fourier analysis in low-resolution data. Two examples of these are a spiky profile (e.g. *AAH1*, Fig. 2B), and a profile with two peaks per cycle (e.g. *CTR3*). Both of these profile types are clearly periodic with a 300-minute cycle, and have a high 300-minute autocorrelation, but do not have a significant 300-minute Fourier component. Finally, to assess the P-value of detection, we compared the measured 300-minute autocorrelation with autocorrelation expected from random (Gaussian distributed) data with no periodicity.

Clustering analysis

The raw expression data was normalized per chip using Genespring v7 and then used for periodicity and cluster analysis. To describe the spatial structure of the temporal

gene expression profiles, we have applied a clustering scheme. To facilitate the comparison of genes with different average expression levels, the temporal profiles of periodically expressed genes were normalized to a common expression level and dispersion. To reduce influence of experimental noise and redundancy of the analysis, we averaged the profiles over three periods. Next, a clustering procedure implementing the k-means algorithm (*13*), with Euclidean distance, was applied to the resulting 12-dimensional dataset. The clustering results revealed three main groups of periodic genes, and the cluster means are displayed using spline-smoothed curves (Fig. 3B). For sentinel-based clustering, the 'find similar' function of GeneSpring v7 was used to determine genes with similar expression profiles (standard correlation >0.9).

Classification of periodic genes

The average expression levels of periodic transcripts was ~1.7-fold higher than that of non-periodic transcripts. This fact may introduce a bias to functional and localization comparisons, since protein function, localization, and other properties such as evolutionary rate are strongly correlated with their expression levels. Therefore, we restricted our comparisons to an expression range, within which the periodicity detection ratio only weakly depends on the expression level. This is a subset of 3,539 genes, whose expression level is between 17th and 84th percentile.

Fluorescence and light microscopy

Yeast cells were rapidly harvested from the fermentor at different time intervals and fixed by the addition of parafomaldehyde to 4%. After fixing for 15 min at 25°, cells were washed with 0.1 M potassium phosphate pH 6.6, and then resuspended in the same buffer and kept at 4°. The fixed cells were visualized using a Nikon Eclipse 90i fluorescence DIC-enabled microscope coupled to a Roper Coolsnap ES monochrome CCD. Cells from 12 time intervals over one cycle were observed and the images representative of the primary differences were selected for inclusion.

Electron microscopy

Samples from six time intervals of the metabolic cycle were prepared for electron microscopy analysis using a slightly modified version of the protocol by R. Wright (*14*). Sections were observed using a transmission electron microscope (Model JEOL 1200 EX) at 20,000-25,000X. Images representative of the primary differences were selected for inclusion.

NMR analysis of metabolites

At each of 12 time intervals, a 540 µL-aliquot of the culture supernatant was taken and added to 60 µL of an internal standard. The internal standard (Chenomx, Edmonton, Alberta, Canada) contained 99.9% D_2O, 0.2% w/v NaN_3 to inhibit bacterial growth, and 5 mM 2,2-dimethyl-2-silapentane-5-sulfonate (DSS) as a chemical shift indicator. The 600 µL sample was placed in a 5mm NMR tube and the ^1H NMR spectra were acquired on a Varian Inova (Palo Alto, CA) 600 MHz NMR spectrometer with the first slice of a NOESY 2D sequence. The spectra were acquired with a 1 sec

presaturation pulse and water suppression during the 200 ms mixing delay. The acquisition time was 4 sec, for a total interpulse delay of 5 seconds. A minimum of 128 transients were collected for each spectrum.

Supplementary Figures

Table S1. The 40 genes with the most similar expression profiles to *MRPL10*.

Corr.	Gene	Description
1.000	MRPL10	mitochondrial ribosomal protein MRPL10 (YmL10)
0.973	MRPL40	mitochondrial ribosomal protein MRPL40 (YmL40)
0.969	RML2	mitochondrial ribosomal protein L2 of the large subunit
0.968	MRPL15	mitochondrial ribosomal protein MRPL15 (YmL15)
0.966	COX10	putative farnesyl transferase required for heme A synthesis
0.965	IMG2	(required for) Integrity of Mitochondrial Genome 2
0.965	MSW1	mitochondrial tryptophanyl-tRNA synthetase
0.965	MHR1	involved in homologous recombination in mitochondria
0.965	MRPL32	mitochondrial ribosomal protein MRPL32 (YmL32)
0.964	ISM1	mitochondrial isoleucyl-tRNA synthetase
0.964	YDR115W	similarity to bacterial ribosomal L34 proteins
0.963	MRPL7	mitochondrial ribosomal protein MRPL7 (YmL7)
0.963	MRPL13	mitochondrial ribosomal protein YmL13
0.962	MAM33	mitochondrial acidic matrix protein
0.961	MNP1	putative mitochondrial ribosomal protein L12
0.960	MRPL11	mitochondrial ribosomal protein MRPL11 (YmL11)
0.959	MEF1	mitochondrial elongation factor G-like protein
0.959	MRP1	mitochondrial ribosomal protein
0.959	CBP3	required for assembly of ubiquinol cytochrome c reductase complex
0.958	MRPL4	mitochondrial 60S ribosomal protein L4
0.958	MBA1	Respiratory chain assembly protein
0.958	ATP11	essential for assembly of a functional F1-ATPase
0.957	RSM19	mitochondrial ribosomal protein of the small subunit
0.956	MST1	mitochondrial threonine-tRNA synthetase
0.956	YGR021W	similarity to M.leprae yfcA protein
0.956	MRPL24	mitochondrial ribosomal protein MRPL24 (YmL24)
0.955	MRPL20	mitochondrial ribosomal large subunit protein YmL20
0.955	MRPL19	mitochondrial ribosomal protein of the large subunit
0.955	MRPL35	mitochondrial ribosomal protein MRPL35 (YmL35)
0.955	MRPL8	mitochondrial ribosomal protein MRPL8 (YmL8)
0.954	YJL213W	similarity to Methanobacterium aryldialkylphosphatase related protein
0.954	OMS1	mitochondrial membrane protein
0.953	MRPS17	mitochondrial ribosomal protein of the small subunit
0.953	YER087W	similarity to E.coli prolyl-tRNA synthetase
0.952	MSD1	mitochondrial aspartyl-tRNA synthetase
0.951	IDH1	Alpha-4-beta-4 subunit of mitochondrial isocitrate dehydrogenase 1
0.951	PET117	cytochrome c oxidase assembly factor
0.950	YDR493W	hypothetical protein
0.949	SLM5	mitochondrial asparaginyl-tRNA synthetase
0.949	MRPS9	probable mitochondrial ribosomal protein S9

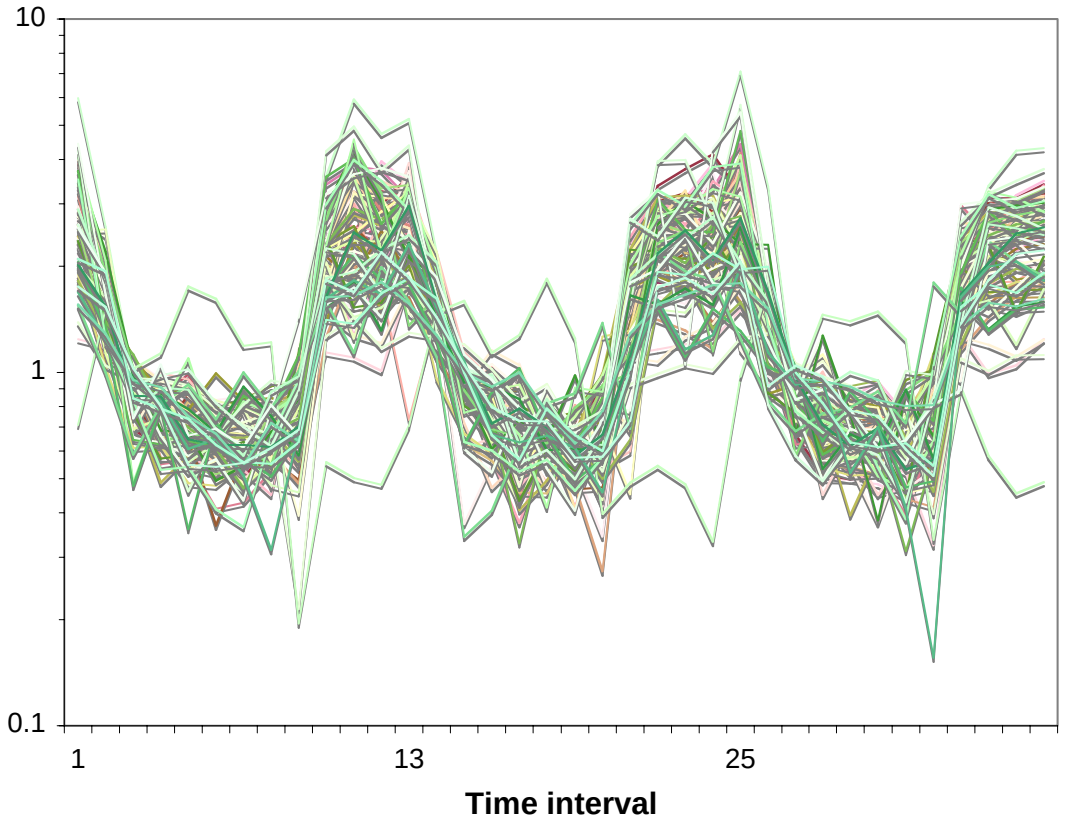

Fig. S1. Temporal expression profiles of the 74 nuclear-encoded mitochondrial ribosomal genes. The one gene (*PPE1*) that has a different expression profile may be misannotated (*15*).

Table S2. The 40 genes with the most similar expression profiles to *POX1*.

Corr.	Gene	Description
1.000	POX1	fatty-acyl coenzyme A oxidase
0.989	ARO9	aromatic amino acid aminotransferase II
0.985	FAA2	acyl-CoA synthetase (fatty acid activator 2)
0.982	CIT3	mitochondrial isoform of citrate synthase
0.981	FOX2	peroxisomal multifunctional beta-oxidation protein
0.981	CTA1	catalase A, peroxisomal
0.974	PXA2	peroxisomal ABC transporter 2
0.972	EHD1	peroxisomal enoyl-CoA hydratase
0.971	PXA1	subunit of a peroxisomal ATP-binding cassette transporter
0.968	IDP3	peroxisomal NADP-dependent isocitrate dehydrogenase
0.968	SUE1	required for degradation of unstable cytochrome c
0.967	TPO4	polyamine transport protein
0.962	ICL2	isocitrate lyase, may be nonfunctional
0.962	CAT2	carnitine O-acetyltransferase, peroxisomal and mitochondrial
0.961	ACS1	inducible acetyl-coenzyme A synthetase
0.959	ARO10	phenylpuruvate decarboxylase
0.951	YIL057C	strong similarity to YER067w
0.949	MDH2	cytosolic malate dehydrogenase
0.949	ATO3	plasma membrane protein
0.948	DBR1	debranching enzyme
0.946	POT1	peroxisomal 3-oxoacyl CoA thiolase
0.946	YCR062W	similarity to Ytp1p protein
0.945	YEL057C	hypothetical protein
0.942	ADH2	alcohol dehydrogenase II
0.941	YKL187C	strong similarity to hypothetical protein YLR413w
0.940	YER121W	hypothetical protein
0.938	SSU1	sensitive to sulfite
0.933	YPR150W	questionable ORF
0.932	QDR3	multidrug transporter
0.932	ADY2	acetate transporter
0.931	SPS19	peroxisomal 2,4-dienoyl-CoA reductase
0.931	FAA1	long chain fatty acyl:CoA synthetase
0.930	YER004W	similarity to hypothetical E.coli and C.elegans proteins
0.923	PRR2	strong similarity to putative protein kinase NPR1
0.922	BAG7	GTPase activating protein (GAP)
0.922	NDE2	mitochondrial external NADH dehydrogenase
0.922	ZPS1	GPI-anchored protein
0.922	FDH1	protein with similarity to formate dehydrogenases
0.918	YLR312C	hypothetical protein
0.917	CSM4	protein required for accurate chromosome segregation during meiosis

Table S3. The 40 genes with the most similar expression profiles to *RPL17B*.

Corr.	Gene	Description
1.000	RPL17B	ribosomal protein L17B (L20B) (YL17)
0.963	RPL6B	60S ribosomal subunit protein L6B (L17B) (rp18) (YL16)
0.963	RPL13A	ribosomal protein L13A
0.958	RPS28B	ribosomal protein S28B (S33B) (YS27)
0.956	RPS26B	ribosomal protein S26B
0.950	SSB2	heat shock protein of HSP70 family, homolog of SSB1
0.949	FCY2	ribosomal protein L34A
0.947	RPS1A	ribosomal protein S1A (rp10A)
0.944	RPL17A	ribosomal protein L17A (L20A) (YL17)
0.944	RPS16B	ribosomal protein S16B (rp61R)
0.943	RPS0B	ribosomal protein S0B
0.940	CYS3	cystathionine gamma-lyase
0.938	RPS7B	ribosomal protein S7B (rp30)
0.935	YOR309C	questionable ORF
0.934	RPL36A	ribosomal protein L36A (L39) (YL39)
0.930	YPL207W	hypothetical protein
0.929	SPE2	S-adenosylmethionine decarboxylase
0.928	ADE5,7	glycinamide ribotide synthetase and aminoimidazole ribotide synthetase
0.926	RPL31B	ribosomal protein L31B (L34B) (YL28)
0.925	MET16	3'phosphoadenylylsulfate reductase
0.923	MPT4	specific affinity for guanine-rich quadruplex nucleic acids
0.923	RPL35A	ribosomal protein L35A
0.922	RPA190	RNA polymerase I subunit 190 (alpha)
0.922	ADE1	phosphoribosyl amino imidazolesuccinocarbozamide synthetase
0.919	PRO1	gamma-glutamyl kinase
0.919	PHO88	membrane protein involved in inorganic phosphate transport
0.919	RPS22A	ribosomal protein S22A (S24A) (rp50) (YS22)
0.918	OGG1	8-oxo-guanine DNA glycosylase
0.918	RPL18A	ribosomal protein L18A (rp28A)
0.918	CTP1	citrate tranporter in mitochondrial inner membrane
0.917	FRS2	phenylalanyl-tRNA synthetase, beta subunit, cytoplasmic
0.917	RPS13	ribosomal protein S13 (S27a) (YS15)
0.917	RPS9B	ribosomal protein S9B (S13) (rp21) (YS11)
0.916	SHM2	serine hydroxymethyltransferase
0.915	IMD3	inosine monophosphate dehydrogenase
0.914	MET8	effector in the expression of PAPS reductase and sulfite reductase
0.913	BEL1	WD repeat protein that interacts with the translational machinery
0.913	NPL3	nuclear shuttling protein with an RNA recognition motif
0.912	RPL8B	ribosomal protein L8B (L4B) (rp6) (YL5)
0.911	RPS18B	ribosomal protein S18B

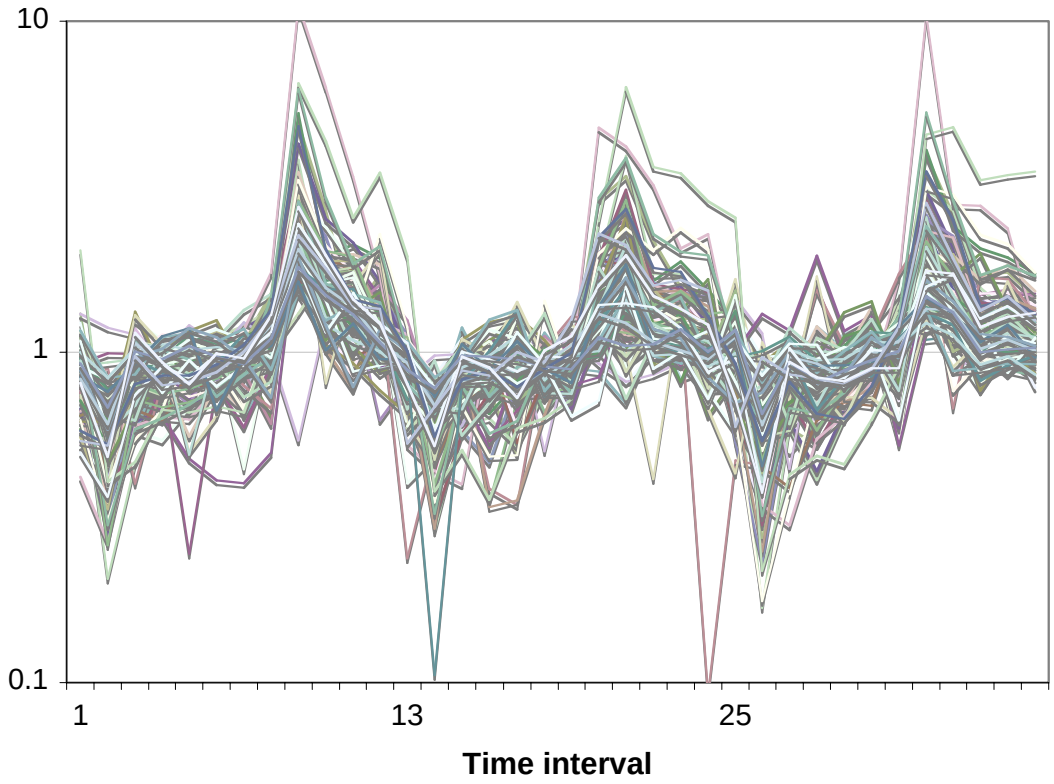

Fig. S2. Temporal expression profiles of 138 annotated cytosolic ribosomal proteins.

REFERENCES

1. F. Sherman, *Methods Enzymol* **350**, 3 (2002).
2. M. S. Longtine *et al.*, *Yeast* **14**, 953 (1998).
3. R. Nash, G. Tokiwa, S. Anand, K. Erickson, A. B. Futcher, *Embo J* **7**, 4335 (1988).
4. R. R. Klevecz, J. Bolen, G. Forrest, D. B. Murray, *Proc Natl Acad Sci U S A* **101**, 1200 (2004).
5. B. P. Tu, A. Kudlicki, M. Rowicka, S. L. McKnight, *data not shown*.
6. L. L. Breeden, *Curr Biol* **13**, R31 (2003).
7. J. R. Walker, J. B. Hogenesch, *Methods Enzymol* **393**, 366 (2005).
8. N. Lomb, *Astrophysics and Space Science* **39**, 447 (1976).
9. J. D. Scargle, *Astrophysical Journal* **263**, 835 (1982).
10. J. H. Horne, S. L. Baliunas, *Astrophysical Journal* **302**, 757 (1986).
11. R. J. Cho *et al.*, *Mol Cell* **2**, 65 (1998).
12. P. T. Spellman *et al.*, *Mol Biol Cell* **9**, 3273 (1998).
13. J. A. Hartigan, M. A. Wong, *Applied Statistics* **28**, 100 (1979).
14. R. Wright, *Microsc Res Tech* **51**, 496 (2000).
15. J. Wu *et al.*, *Embo J* **19**, 5672 (2000).